COMPDYN 2021
8th ECCOMAS Thematic Conference on
Computational Methods in Structural Dynamics and Earthquake Engineering
M. Papadrakakis, M. Fragiadakis (eds.)
Streamed from Athens, Greece, 27–30 June 2021

SIMPLE AND COMPLEX MODELLING OF SEAT-TYPE ABUTMENT-BACKFILL SYSTEMS

Ioannis G. Mikes[1], Andreas J. Kappos[1]

[1] Department of Civil Infrastructure and Environmental Engineering, Khalifa University
Abu Dhabi, United Arab Emirates
e-mails: ioannis.mikes@ku.ac.ae, andreas.kappos@ku.ac.ae

Abstract

The response of the seat-type abutment-backfill system under a dynamic excitation and its contribution to the structural system of the entire bridge is usually ignored in practice in Europe, since the designers prefer providing joint gap sizes larger than the required for the design earthquake. In the high seismic hazard areas of the US, various versions of Caltrans Guidelines prescribe a relatively simple way to account for the abutment – backfill interaction. However, the design of Caltrans abutments is based on the 'fully sacrificial' approach, wherein the backwall 'shears off' at an early stage, while in other countries the detailing of the deck-abutment interface is such that a plastic hinge forms at the base of the backwall which is detailed for ductile behaviour. In all cases, if assessment of the bridge safety beyond the design earthquake is sought (e.g. in fragility analysis), it is essential to properly account for the response of the bridge when the end joint is closed.

This paper focuses on seat-type abutments with backwall hinging. In a practical context, a 'simple' model in this case consists of a spring-gap element that models the entire abutment-backfill system, while a 'complex' model includes explicit modelling of the abutment using beam-column elements, and of the backfill behind it using one or multiple soil springs. For dynamic response-history analysis, dashpots are also needed for modelling radiation damping. The issues of the number and the arrangement of the spring-dashpot systems and their nonlinear constitutive laws are addressed herein and several configurations are studied. SAP 2000 is used for analysing a typical overpass bridge with seat-type abutments and joints in both the longitudinal and transverse directions, for a number of spectrum compatible records. A series of pushover analyses of the 'complex' model are also carried out; their output can be used to define the (single) spring properties of the simple model. Interesting conclusions are drawn, both with regard to the spring configuration and to the difficulties in combining the various nonlinear elements in SAP 2000.

Keywords: Bridges, Abutment, Backfill, Seismic design

1 INTRODUCTION

While in integral abutment bridges it is now customary to model the stiffness of the backfill soil (and indeed the forthcoming new Eurocode 8-2 makes mandatory to model the effect of interaction between soil and abutments in such bridges), in the case of seat-type abutments this interaction is usually ignored in practice. In a number of European countries, designers prefer to provide end joint gaps substantially larger than the expected seismic displacement of the deck under the design earthquake, so that the joint remains open and the contribution of the backfill can be ignored. In various versions of Caltrans' Guidelines [1], which are implemented in the high seismic hazard regions of the US, seat-type abutments backfill systems in straight bridges are taken into account in a simplified way. Specifically, in the longitudinal direction, the simplified recommendations of the current Caltrans are based on the work of Shamsabadi et al. [2], which, in turn, is based on large-scale abutment tests at UCLA. For the transverse direction a nominal spring stiffness is suggested; this stiffness is not directly correlated to the actual stiffness of the shear keys or the abutment-backfill system, but it is simply meant to suppress unrealistic (?) response modes that would emerge in the transverse direction in the case of a completely unrestrained deck end [1]. Modelling of seat-type abutments is reviewed in the reports of Aviram et al. [3] and the more recent one by Omrani et al. [4], where there are also practical guidelines for modelling in SAP 2000 and OpenSees, respectively. However, Caltrans and the aforementioned reports refer to the 'fully sacrificial' backwall approach, i.e. a backwall that 'shears off' almost immediately after gap closure.

In this paper, the behaviour of seat-type abutment-backfill systems with hinging backwall and exterior shear keys is examined using 'simple' models consisting of one spring-gap element at each end that models the entire abutment-backfill system, and 'complex' models including explicit modelling of the abutment using beam-column elements, and of the backfill behind it using one or multiple soil springs. For a real bridge selected as a case study, in the longitudinal direction, nonlinear static analyses of various configurations of this system are conducted and are compared with a similar backwall-backfill system designed following the 'fully sacrificial' approach. In both the longitudinal and transverse directions, nonlinear response history analyses for different levels of seismic action are caried out to investigate the feasibility of the aforementioned configurations and their effect on the response of the entire bridge. The effect of the joint gap size is also investigated herein and several conclusions are drawn, regarding the importance of accounting for the deck-abutment-backfill interaction and the modelling challenges that it poses.

2 OVERVIEW OF THE CASE-STUDY BRIDGE

The studied bridge (called T7) is an actual overpass of Egnatia Motorway in northern Greece, designed by a German firm and overall representative of modern bridge design practice in Europe. It is a three-span concrete structure, designed for earthquake according to the 2000 Greek national seismic code (EAK2000), very similar to the then current draft of Eurocode 8-2. The total length of the bridge is 99 m, consisting of a 45 m central span and two 27 m outer spans, while the longitudinal slope of its axis is equal to 7%. The deck consists of a 10 m wide prestressed concrete box girder section with a continuously changing cross section along the length of the bridge. The two piers of the bridge have a circular cross section, with a diameter of 2 m and are monolithically connected to the deck; their clear heights are 5.94 m and 7.93 m (Fig. 1).

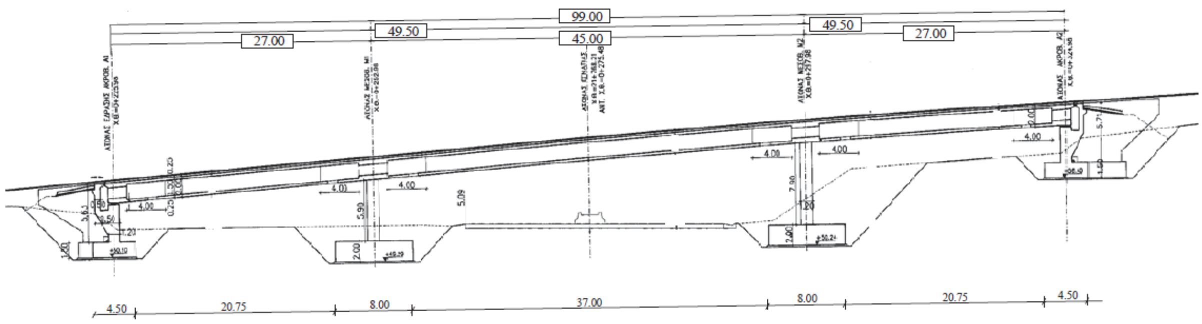

(a)

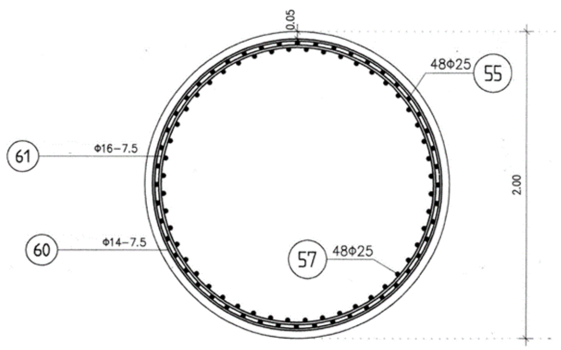

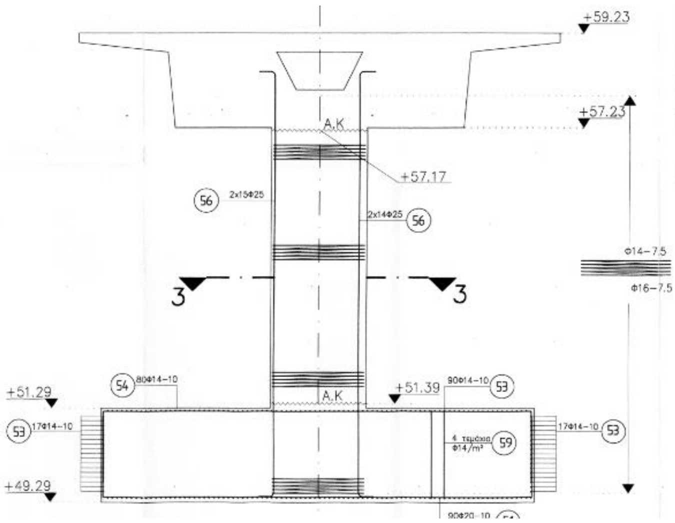

(b) (c)

Figure 1: (a) Longitudinal section of the bridge, (b) Pier section, (c) Section close to pier

The deck is supported on seat-type abutments (Fig. 2), which include backwall, wingwalls, and external shear keys, through two elastomeric bearings with dimensions (mm) equal to 350×450×136. The total heights of the abutments are equal to 5.63 m and 5.71 m, while the height of both backwalls is 2.45 m. The deck is separated from the seat-type abutments with joints of 100 mm in the longitudinal direction and 150 mm in the transverse direction.

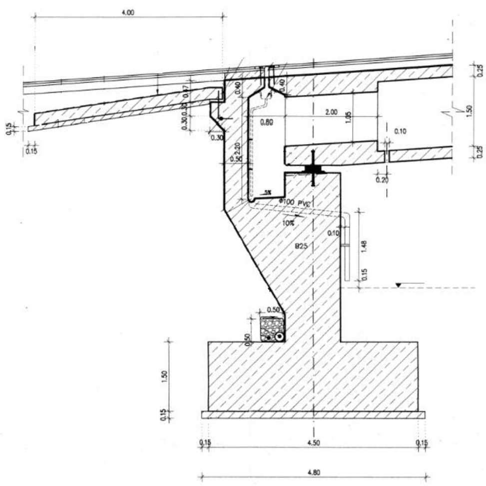

Figure 2: Section at the abutment

The piers, as well as the abutments, rest on surface footings (due to the relatively firm soil). The pier footings are 9.0 m × 8.0 m × 2.0 m, while the abutment footings are 12.0 m × 4.5 m × 1.5 m. The soil in the bridge area mainly consists of moderately stiff clay formations, corresponding to soil class C according to Eurocode 8 [5]. In the absence of measured data, a shear wave velocity V_s = 300 m/s was assumed for modelling the properties of clay, while its specific weight was taken as $\gamma = 20$ kN/m^3.

3 FINITE ELEMENT MODELLING OF THE BRIDGE

3.1 Modelling of concrete members

The bridge was modelled using the broadly used SAP 2000 software [6] as shown in Fig. 3. The prestressed deck is deemed to remain elastic during the seismic event and it was modelled as a non-prismatic section, varying along its length, to take into account its changing shape along the longitudinal axis. The inelastic behaviour expected to develop at the bridge piers was modelled with plastic hinges at both ends of each pier (monolithic connection to the deck). SAP 2000 uses a moment-rotation curve for its plastic hinge elements, which was defined on the basis of the pertinent moment-curvature diagram. The length of the plastic hinges was calculated as the weighted average of two relationships available for piers [7], [8]:

$$L_{pl} = 0.08L_s + 0.022d_{bl} f_y \tag{1}$$

$$L_{pl} = 0.6D\left[1+\frac{1}{6}\min\left(9;\frac{L_s}{D}\right)\right] \tag{2}$$

where L_{pl} is the calculated plastic hinge length, L_s is the shear span of the pier, d_{bl} is the diameter of the longitudinal bars, f_y is the yield strength of concrete and D is the diameter of the pier. A weighting factor of 0.7, is selected for relationship (2) since it was derived from numerous experimental results and was specifically created for circular columns, whereas relationship (1) is recommended for general use.

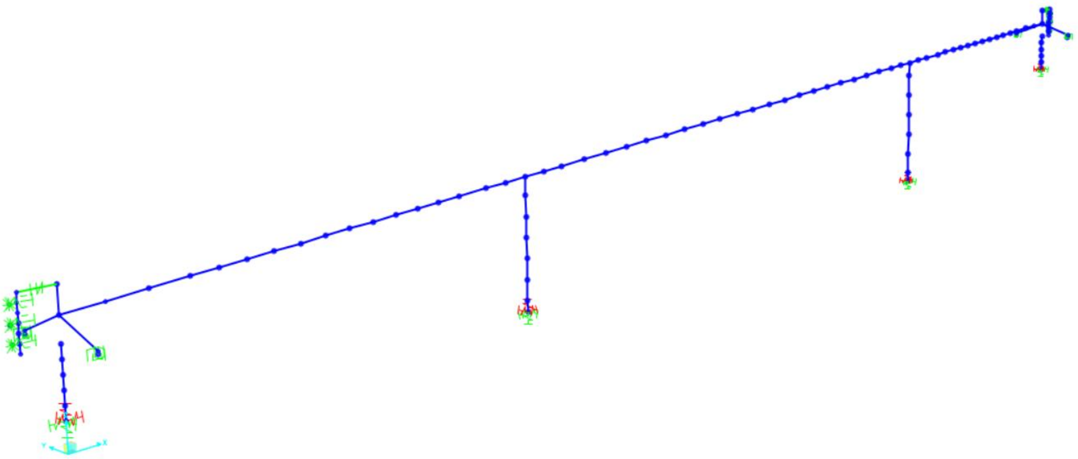

Figure 3: Finite element model of the bridge

Moment-curvature (M-φ) curves are obtained at every pier end, using the section analysis software AnySection [9] for the axial load $N_{G+0.3}$. The constitutive models of the materials used in section analysis were the model by Mander et al. as adapted by Paulay & Priestley [7] for confined concrete, the nonlinear model of EN1992-1 [10] for unconfined concrete and the model of Park and Sampson [11] for reinforcing steel. To define the (apparent) yield point, the M-φ curves were bilinearised by adopting the criteria of 15% strength drop and equality of areas under the "exact" and the bilinear curve (equal energy absorption).

The horizontal shear behaviour of the (common) elastomeric bearings was considered bi-linear, while in the other directions the bearings are considered to respond linearly. All the relevant stiffnesses, namely initial and post-yield horizontal shear stiffness ($K_{h,el}$ and $K_{h,pl}$), flexural stiffnesses (K_{bx} and K_{by}) and axial stiffness (K_v) were calculated according to [12].

Soil-structure interaction at the foundations of the piers and the abutments of the bridge was taken into account, utilising equivalent linear springs at the bases of the respective beam-column elements of the model. The stiffness values of these springs were calculated according to Mylonakis et al. [13].

The seat-type abutment-backfill system was modelled in detail, as its behaviour is the main focus of this study. This 'complex' (in a practical design context) abutment-backfill model is depicted in Fig. 4. It consists of separate beam-column elements which represent the stem wall and the backwall, while the behaviour of the backfill soil was modelled using multiple pairs of springs and dampers (Kelvin-Voigt elements) distributed along the height of the stem wall and the backwall. A moment-curvature (M-φ) curve was derived from AnySection for the expected plastic hinge at the base of the backwall, while the estimated length of this plastic hinge was calculated from the relationship of Biskinis [14], developed for concrete walls:

$$L_{pl} = 0.1L_s + 0.2h \tag{3}$$

A gap element was placed between the top of the backwall and the end of the deck; several initial gap sizes were used, to investigate the effect of the gap size on the response of the bridge. The constitutive models used for the springs and dashpots representing the backfill soil are described in the next section.

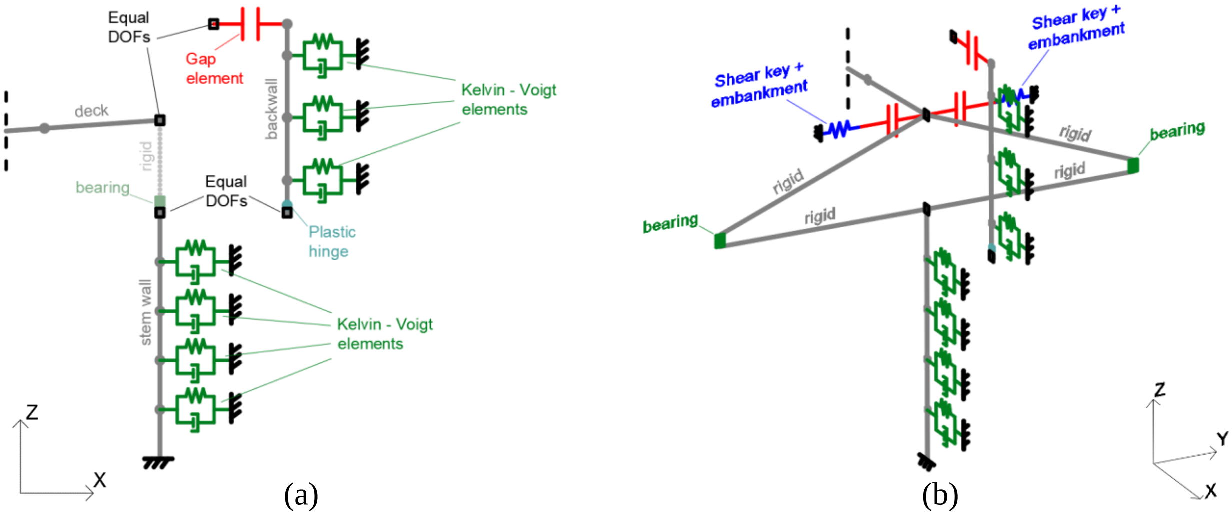

Figure 4: (a) Longitudinal section and (b) 3-d view of the 'detailed' abutment-backfill model

3.2 Modelling of the backfill soil behaviour

The radiation damping and the hysteretic behaviour of the backfill soil in the longitudinal direction are modelled with the use of multiple spring-dashpots along the abutment, each of which consists of a viscous damper and a nonlinear spring (called "nonlinear link element" in SAP 2000) placed in parallel, as shown in Fig. 4. The effect of the number of these pairs and their position in the abutment-backfill was investigated through a series of non-linear static (pushover) analyses.

The closed-form relationship recently proposed by Khalili-Tehrani et al. [15] was adopted as the backbone curve of the nonlinear backfill springs. This relationship is based on the log-spiral hyperbolic (LSH) model proposed by Shamsabadi et al. [16], which was verified against large-scale experiments on backwall – backfill systems with different types of soil. The relationship is given by:

$$F(y) = f_{\delta} \frac{a_r y}{\hat{H} + b_r} \hat{H}^{n} \tag{4}$$

where f_{δ} is a function of the wall – soil interface friction angle, a_r and b_r express backfill capacity and wall displacement at capacity, respectively, and $\hat{H}$ is the normalised value of the wall height.

The above hyperbolic relationship and its parameters were derived from a calibration of multiple experimental results, which were conducted using a 1.7m high backwall specimen, pushed horizontally against backfill of various soil types, considering it a typical sacrificial backwall with almost no shear resistance, i.e. designed to break almost immediately after gap closure, as per the relevant Caltrans provisions [1] (also found in older Caltrans guidelines). As a result, the behaviour of the abutment – backfill was governed by the passive pressures of the backfill soil developing uniformly along the height of the wall. However, in the studied bridge, the backwall is designed to form a plastic hinge at its base. Consequently, after gap closure, it does not shear off but it has a predominantly flexural response, and the backfill soil near the top of the wall deforms more than at its base. Therefore, in the longitudinal direction, the abutment was modelled with separate frame elements representing the stem wall and the backwall, while the backfill soil was modelled with multiple springs to better capture the differing soil deformation along the backwall height.

For the implementation of (4), a dense granular backfill soil, typically suggested by the pertinent codes/guidelines (e.g. [1]) is considered, with $\varphi = 40^{o}$, $c = 0$, $\gamma = 20 kN/m^3$, soil strain at 50% of the ultimate stress $\varepsilon_{50} = 0.0035m$ (according to Shamsabadi et al. [16] for a similar type of soil), $\nu = 0.35$ and ultimate deformation equal to $0.05H_{bw} = 0.1225m$, where H_{bw} is the height of the backwall; the value of $0.05H_{bw}$ is a common estimation of ultimate deformation for granular backfill soil, derived from large-scale experiments [15], [16].

The nonlinear link provided by SAP 2000 is a multilinear one, hence the previously calculated hyperbolic curve was converted to a quadrilinear approximation. Furthermore, to capture the full-range behaviour of the system, a final descending branch was added to this quadrilinear curve, based on a linear approximation of experimental descending branches for granular soils found in Cole & Rollins [17]; both curves are presented in Fig. 5. In the absence of other options, the compression-only “Concrete” hysteresis model, available in SAP 2000, was adopted as the hysteresis rule of the nonlinear backfill springs.

Last, the dashpot coefficient of the viscous dampers was estimated based on the work of Mylonakis et al. [13] which refers to footings rather than backwalls; so an adjustment was made (as also done in [18]) to account for the fact there is no soil above the backwall. The estimated dashpot coefficient was found to be equal to 13.5 MN s/m.

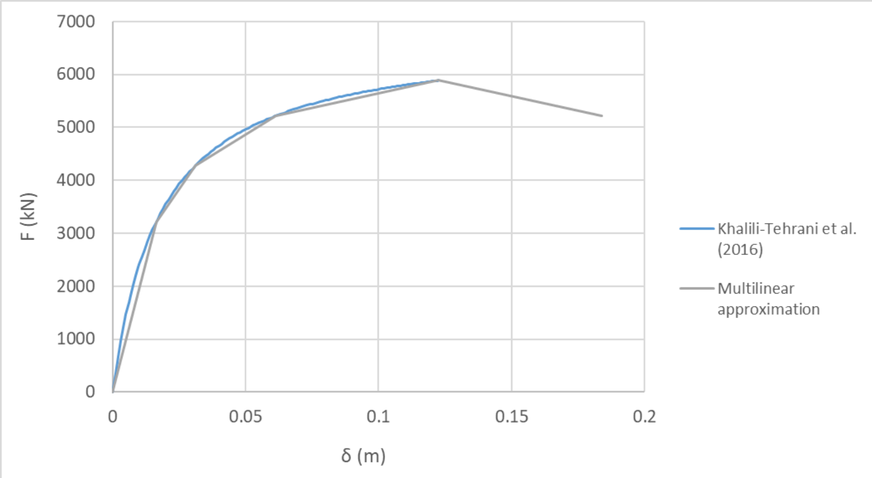

Figure 5: Backfill hyperbolic force-deformation curve according to Khalili-Tehrani et al. [15] and its multi-linear approximation made herein

In the transverse direction, it is considered that the external shear keys of the bridge are practically rigid and remain elastic (which was indeed the case here), and the abutment-backfill system was modelled as a pair of p-y springs which represent the bridge-embankment interaction in the transverse direction, according to the model of Xie et al. [19]. This model, which was derived from multiple 3-D continuum finite element analyses of abutment-backfill models verified against the recorded response of Painter Street Bridge during the 1992 Petrolia earthquake, provides closed-form relationships for the calculation of the ultimate embankment capacity at top of the 3D embankment in the transverse direction ($\Sigma p_{ult,T}$), the value of the embankment displacement that corresponds to 50% of $\Sigma p_{ult,T}$ ($y_{50,T}$) and the value of the transverse secant stiffness at $y_{50,T}$ ($K_{s,T}$). However, no relationship for the calculation of the embankment displacement at $\Sigma p_{ult,T}$ or the estimation of the stiffness when the displacements are larger than $y_{50,T}$ is provided in [19]. In view of this, it was assumed that the full force – deformation curve in the transverse direction is a bilinear one and that the slope of the second branch of this bilinear curve is equal to about 20% of $K_{s,T}$. The bilinear curve that was finally derived is shown in Fig. 6, using the same backfill soil properties which have already been described for the longitudinal direction.

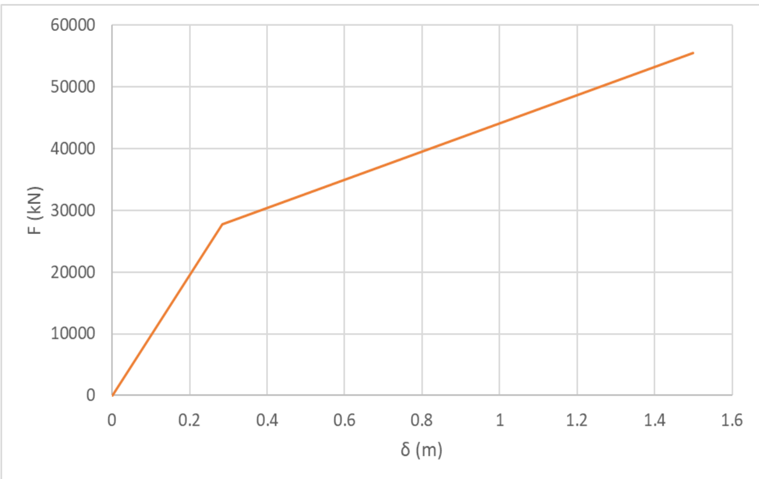

Figure 6: Embankment bilinear force-deformation curve in the transverse direction, based on the model of Xie et al. [19]

4 NONLINEAR ANALYSIS OF THE BRIDGE

4.1 Nonlinear static (pushover) analysis of the abutment-backfill system

In order to investigate the rather complex inelastic behaviour of the abutment-backfill system in the longitudinal direction, before integrating it into the entire bridge model, multiple pushover analyses of different configurations of the system in the longitudinal direction were conducted. The main goals of these analyses were to define the importance of the contribution of the backfill soil after gap closure, to investigate the effect of the number and the positions of soil springs and dashpots and, finally, to compare the behaviour of backwalls which form a plastic hinge at their base with that of 'fully sacrificial' (Caltrans type) backwalls which 'shear off' as soon as the joint gap closes.

The first issue to be addressed is whether the contribution of the lower part of the backfill, i.e. the area behind the stem wall, should be taken into account. In order to investigate the influence of this area, two additional analyses were conducted; one of the abutment alone, without any contribution from the backfill, and one with the lower part of the backfill considered. The respective models are shown in Fig. 7b and 7c. and the resistance curve (i.e. base shear vs displacement at the top of the backwall) is depicted in Fig. 8 and compared with the model which has springs along the entire height of the abutment (Fig. 7a). It is clear that the contribution of the examined part of the backfill is negligible and hence, in the following analyses, only the part of the backfill behind the backwall is considered. This result is anticipated, since the very high stiffness of the stem wall results in little deformation of the springs attached to it, consequently leaving them almost inactive.

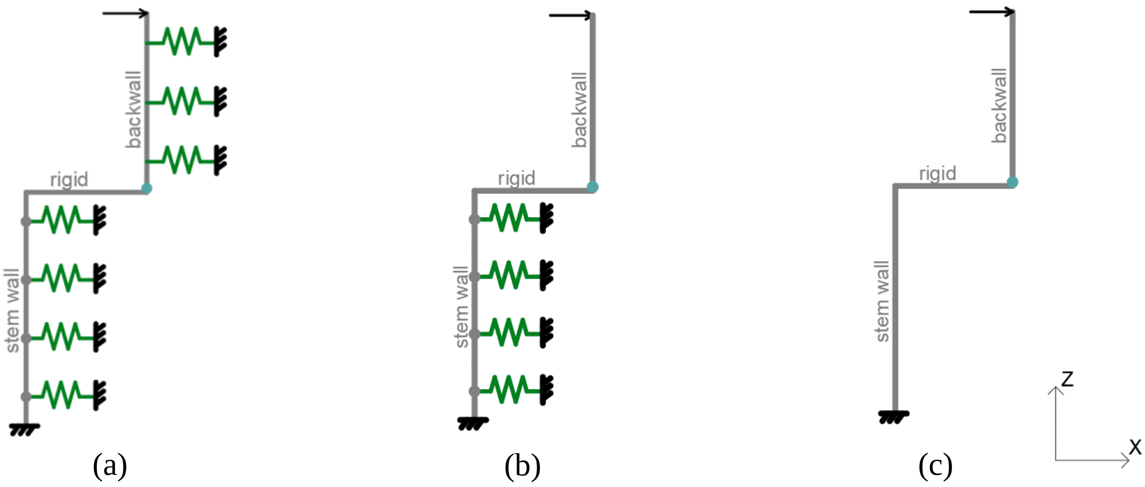

Figure 7: Longitudinal abutment model: (a) with backfill soil springs behind the entire abutment (b) with backfill soil springs behind the stem wall, (c) without backfill soil springs

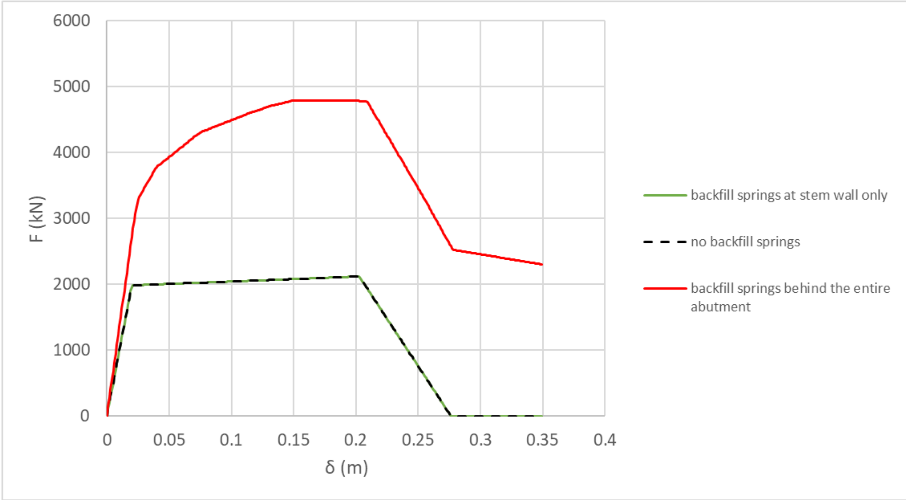

Figure 8: Resistance curve of the abutment with backfill soil springs behind the stem wall, behind the entire abutment and without backfill soil springs

The next issue addressed was the effect of the position and the number of the backfill springs along the height of the backwall. Some of the configurations explored are depicted in Fig. 9; note that in the multiple spring configurations the influence area of each spring is the same. From the resulting resistance (pushover) curves in Fig. 10, it is clear that the number of the springs does not affect the abutment-backfill behaviour significantly, while for 3 springs or more, hardly any difference is observed in the pushover curves, except for the descending branch that follows the failure of the backwall. This difference is caused by the way that the strength drop of the backwall is modelled in the software due to different discretisation of the frame element of the backwall in each case, since the backwall element is divided at each of its connections with the springs; namely, the shorter an element is, the more it is capable of capturing an abrupt strength drop [20]. However, in the case that a single spring is used, placing it at the top of the backwall seriously overestimates the maximum strength of the backfill by almost 60%. It is stressed here that the springs do not contribute to the response of the system in the same way; the closer a spring is to the top of the backwall, the earlier it reaches its maximum strength (Fig. 11), due to the hinging at the base.

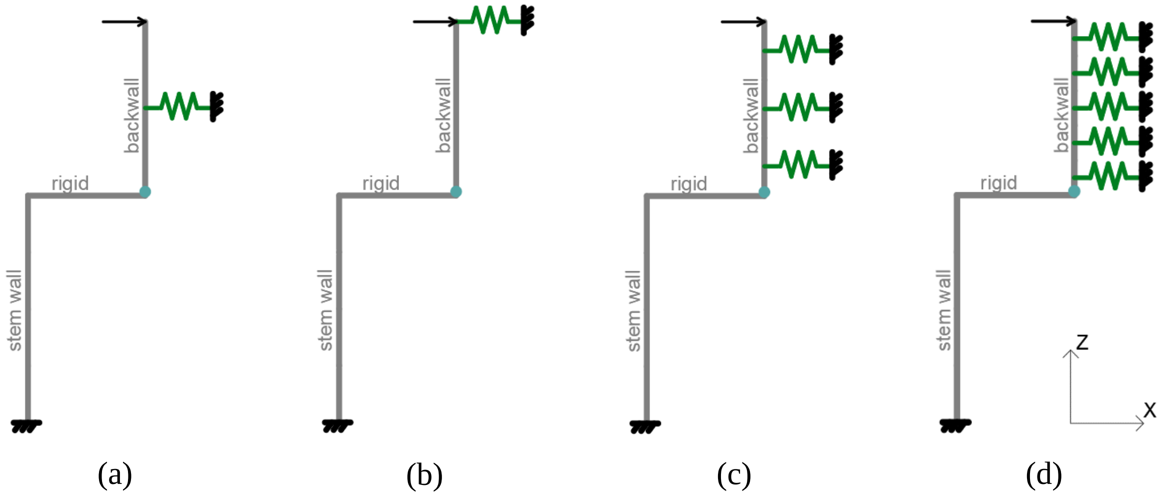

Figure 9: Longitudinal abutment model with: (a) a single backfill soil spring in the middle of the backwall, (b) a single backfill soil spring at the top of the backwall, (c) 3 springs along the height of the backwall, (d) 5 springs along the height of the backwall

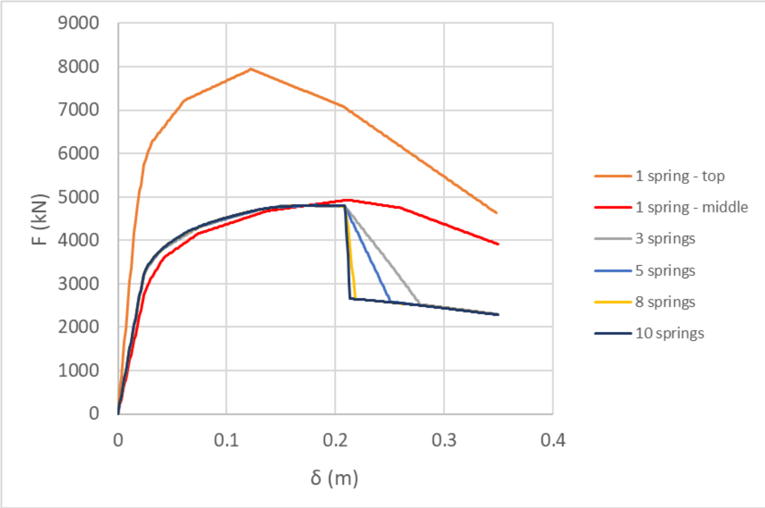

Figure 10: Resistance curves for various numbers of distributed backfill soil springs along the height of the backwall and for a single spring at the top of the backwall

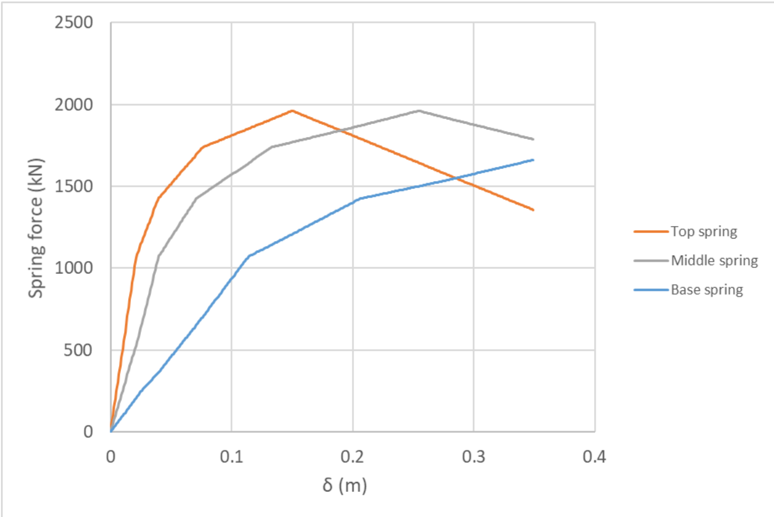

Figure 11: Axial forces developed at the backfill soil springs during the pushover analysis of the abutment-backfill system in the case of 3 used springs along the height of the backwall (Fig. 9c)

The case of the ‘fully sacrificial’ backwall with no shear resistance that shears off right after the gap closure with a lateral force applied at its top, was also examined with the use of a backwall model with a roller support at its base, as shown in Fig. 12a. As seen in Fig. 12b, in this case each of the backfill soil springs contributes equally to the response of the system, meaning that a model which consists of a single spring would be enough for modelling the behaviour of the entire abutment-backfill system adequately. The maximum contribution of the backfill soil springs in the case of the ‘fully sacrificial’ backwall is larger by 15% than in the case that the backwall yields and eventually fails in flexure. The ‘fully sacrificial’ backwall has also higher initial stiffness but it develops its maximum strength at a smaller displacement (Fig. 13). These results can be attributed to the fact that in the case of the ‘fully sacrificial’ backwall every spring along the backwall height is activated simultaneously from the beginning, contrary to the case of the backwall with the plastic hinge at its base.

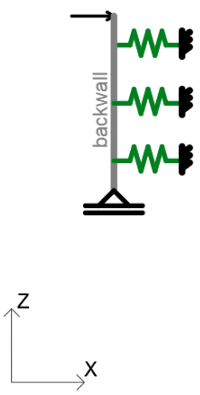

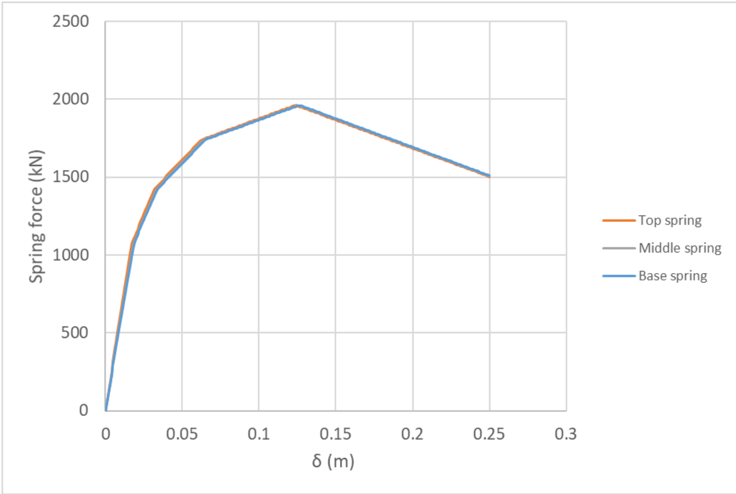

(a) (b)

Figure 12: (a) Longitudinal backwall model with no shear resistance ('fully sacrificial') and 3 backfill soil springs along its height, (b) axial forces developed at the backfill soil springs during the pushover analysis of the 'fully sacrificial' backwall-backfill system in the case of 3 used springs along the height of the backwall (Fig. 12a)

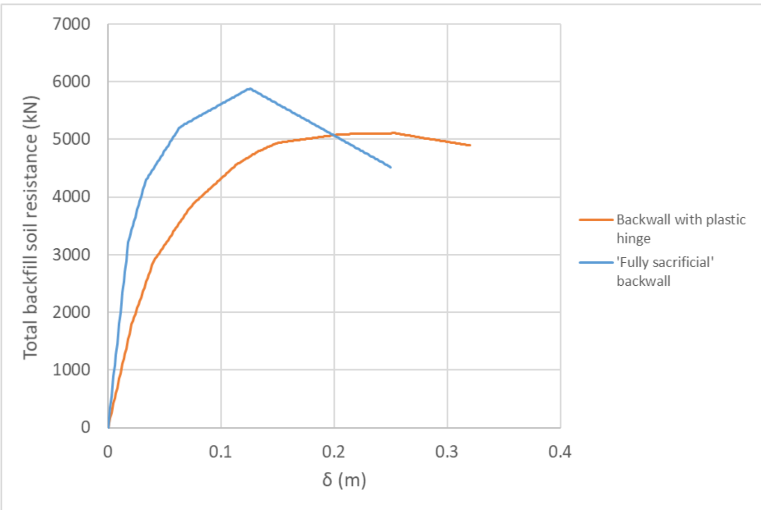

Figure 13: Total contribution of the backfill soil springs in the pushover analyses of backwall with plastic hinge formed at its base and 'fully sacrificial' backwall

4.2 Nonlinear static (pushover) analysis of the bridge model

Having compared the spring configurations that represent the abutment-backfill system, nonlinear static (pushover) analyses of the entire T7 bridge model were conducted, for both the 'fully sacrificial" backwall case and the backwall with a plastic hinge formed at its base. Simple spring configurations (such as a single nonlinear spring for the case of the 'fully sacrificial' case) and more complex models, including detailed modelling with nonlinear beam-column elements representing the abutment and nonlinear springs along the height of the backwall, which represented the backfill soil were used. Five longitudinal joint gap sizes, namely 0 cm, 2.5 cm, 5 cm, 7.5 cm and 10 cm were explored, to study the influence of the gap size. The results are given in Fig. 14 and Fig. 15. The total base shear after gap closure is 23.5% and 30% larger than in the case without gap closure for the 'fully sacrificial' and the backwall with a plastic hinge at its base, respectively.

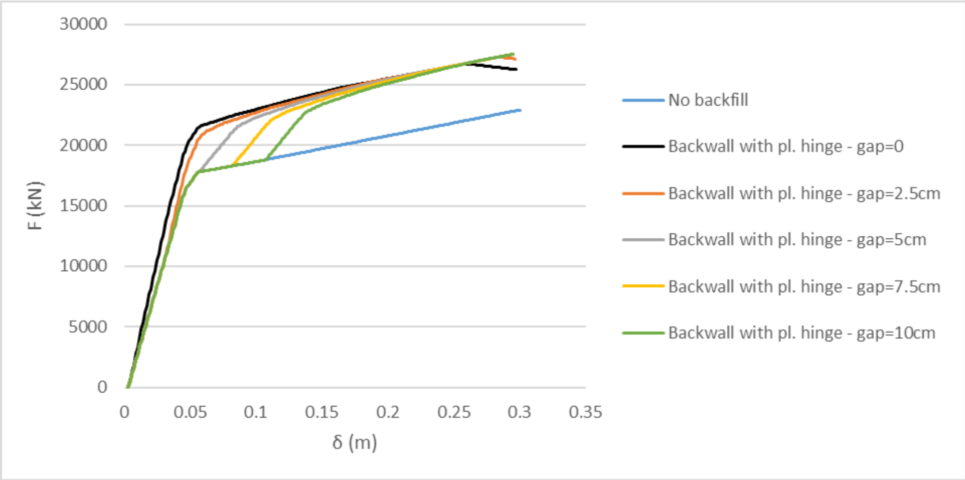

Figure 14: Resistance curves of the entire bridge with ‘detailed’ abutment-backfill model and backwall with plastic hinge at its base in the longitudinal direction, for various joint gap sizes

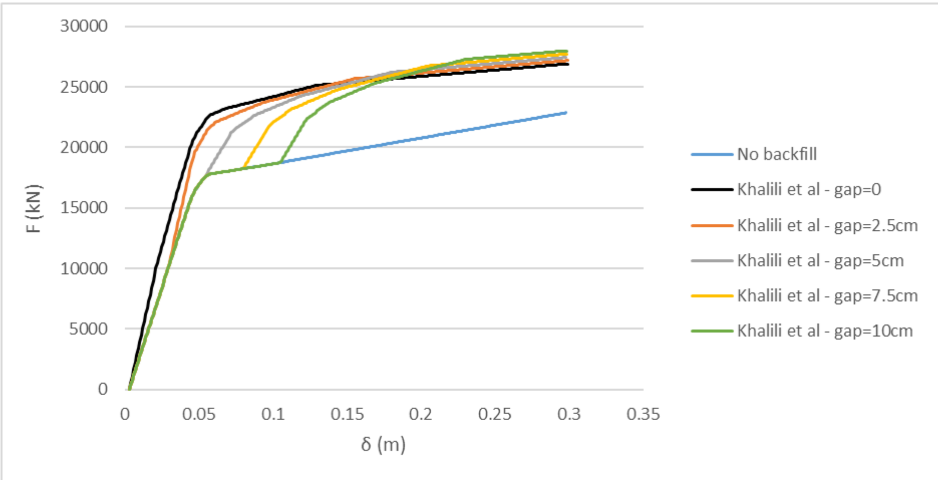

Figure 15: Resistance curves of the entire bridge with single spring according to Khalili-Tehrani et al. [15] representing a ‘fully sacrificial’ backwall in the longitudinal direction, for various joint gap sizes

The effect of simple or complex modelling of the abutment-backfill system can be seen in Fig. 16, where both the detailed and the single-spring model are used to derive resistance curves for the bridge, and these are compared with the detailed (multi-spring) model and the reference case where the abutment-backfill system is ignored (which is the situation prior to gap closure). It is clear (and expected) that when the single spring is defined from the analysis of the abutment-backfill system, the detailed and the simple model produce practically identical curves; however, when the single spring is based on the Khalili et al. [15] model, which corresponds to the case of a shearing-off backwall, the simple model overestimates the strength of the system for the reasons discussed earlier in the paper. Regarding the effect of gap size, the contribution of a shearing-off backwall and a backwall that forms a plastic hinge at its base were very similar for all examined joint gap sizes.

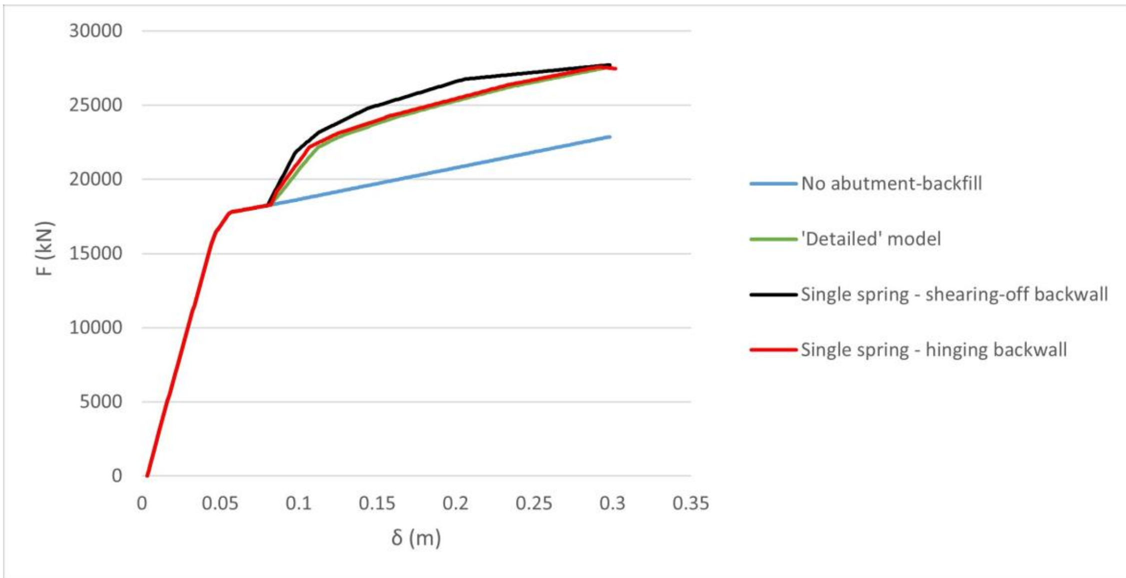

Figure 16: Comparison of the resistance curves of the entire bridge in the longitudinal direction, modelled with ‘detailed’ and ‘simple’ (single spring) model representing either a ‘fully sacrificial’ backwall and a back-wall with plastic hinge at its base, for joint gap size equal to 7.5 cm.

4.3 Nonlinear response history analysis

The nonlinear dynamic response of the bridge was studied to better understand its overall dynamic behaviour and to identify modelling issues that should be further addressed. For the dynamic response history analysis, the bridge is subjected to a set of artificial accelerograms scaled to various levels of intensity, multiples of the design seismic action (0.16g, 0.32g and 0.48g, considering soil class C according to Eurocode 8, but assuming that T_D = 4s instead of T_D = 2s suggested by EC8, as a more representative value of high seismicity regions [21], [22]). In the longitudinal direction, 3 pairs of nonlinear spring and dashpots are used to represent the backfill, while in both directions separate gap elements are used.

The issue of modelling the joint gap was one of the focuses of the investigation. In SAP 2000, gaps are modelled with a separate element, which has zero stiffness when it is open and a user-defined stiffness value when it is closed. The latter value is difficult to define in a way such as to avoid numerical instabilities and to appropriately capture the force transfer between the elements which are adjacent to the gap during response history analysis; this is known from the literature [23] and has also been observed in the analyses conducted for the present work. According to Kim & Shinozuka [23], the stiffness of the gap element should not be larger than 1000 times the stiffness of the adjacent elements in order to avoid numerical instabilities. After conducting preliminary response history analyses of the examined bridge model, it was found out that the response quantities are significantly different when the gap element stiffness is equal to 100 times the stiffness of the adjacent elements or lower from those for gap element stiffness 1000 times the stiffness of the adjacent elements or larger. It was decided to set the gap stiffness equal to 1000 times the initial stiffness of the adjacent elements. However, in a nonlinear analysis, the stiffness of the adjacent elements varies with time, and numerical stability is not achieved in every response history analysis. Moreover, the existence of the gap element results in large analysis duration which becomes even larger as the level of the input ground motion increases and, most importantly, the time step at which the base of the backwall yields is very different even for very small differences in the gap element stiffness or the considered initial gap. The use of a nonlinear spring with a backbone curve that starts with a zero slope would be an alternative solution to avoid all the aforementioned problems. This solution was indeed utilized in the nonlinear *static* analyses with the 'simple' single-spring model; however, in the *dynamic* response history analyses with SAP 2000, it could not be implemented, since no compression-only hysteresis model provided by the software is compatible with such a backbone curve.

Some results of the analyses in the longitudinal and the transverse direction are plotted in Figures 17 and 18. In both directions, the deformation of the upper backfill-soil spring, the bearing deformation and the plastic rotations of the pier are depicted for various gap sizes and for the three selected levels of earthquake intensity. In the longitudinal direction, the derived backwall plastic rotations are also shown.

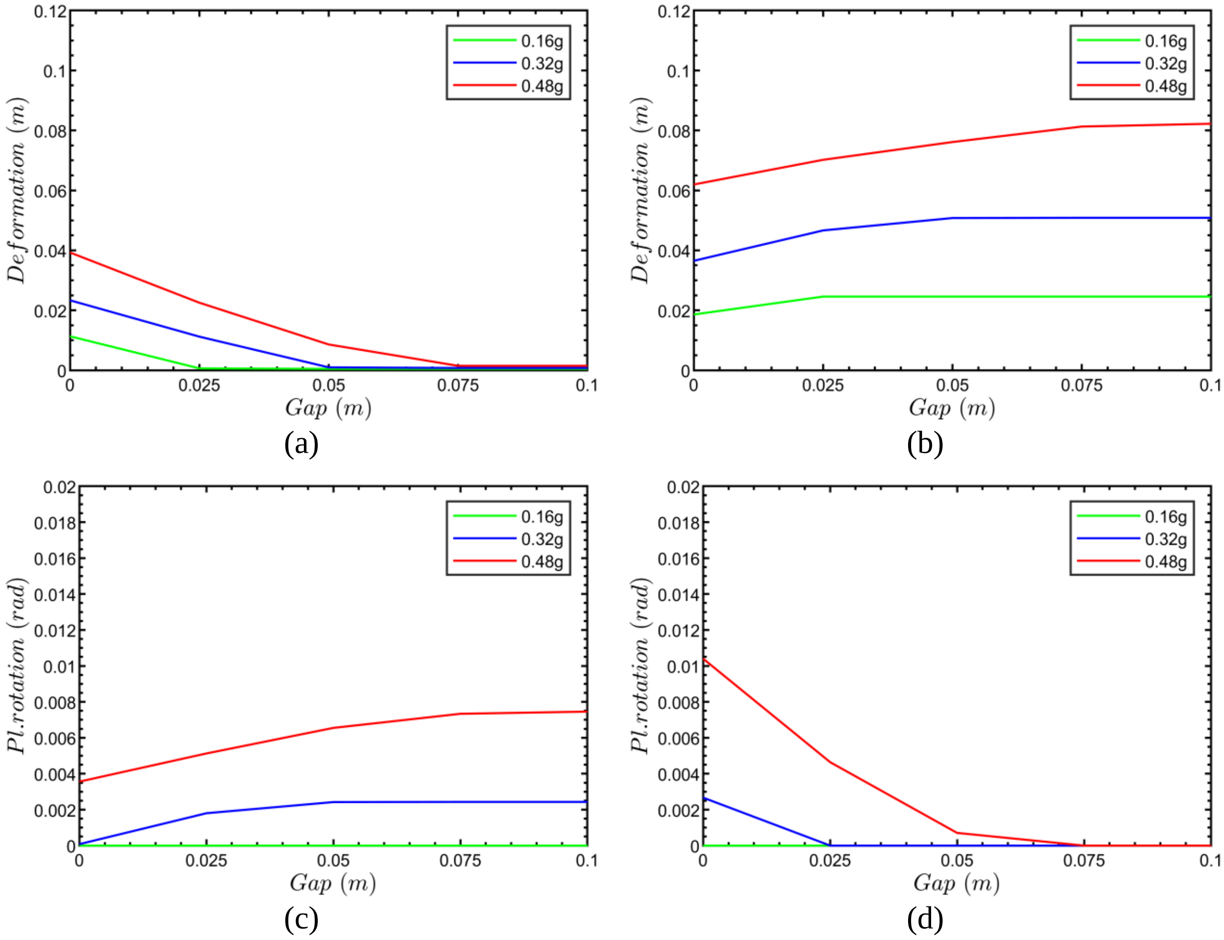

Figure 17: Longitudinal direction: Effect of gap size on: (a) the maximum deformation of the upper backfill spring, (b) the maximum bearing deformation, (c) the maximum pier plastic rotation and (d) the maximum backwall plastic rotation for 3 levels of ground motion

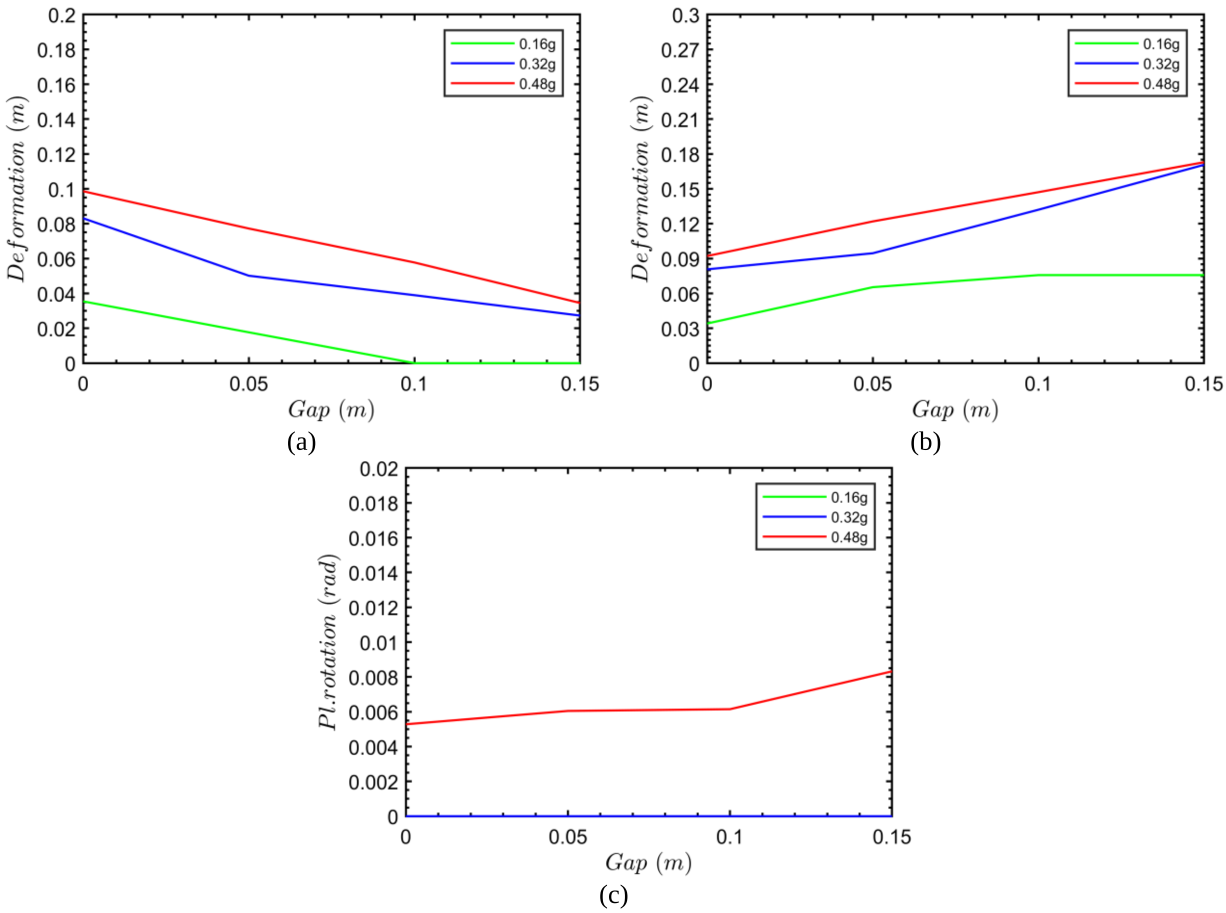

Figure 18: Transverse direction: Effect of gap size on: (a) the maximum deformation of the spring that models the shear key and the embankment resistance, (b) the maximum bearing deformation and (c) the maximum pier plastic rotation for 3 levels of ground motion

The results indicate the importance of accounting for the abutment-backfill system in both directions and the fact that small gap sizes may alter the response of the entire bridge significantly, mainly in cases of high seismic intensities. As expected, the abutment-backfill system is activated more when the gap size is small, and this emerges as beneficial for the piers and the bearings which sustain less damage. Bearings are affected more than piers, particularly in the transverse direction, where an initially closed gap results in approximately 50% decrease of the bearing deformation with respect to 15 cm gap, for ground motion equal to twice the design earthquake. Longitudinal gap sizes larger than 7.5 cm (which is close to the 10 cm gap selected by the designer of the actual bridge), do not make any noticeable difference compared to larger ones, since the displacements in the longitudinal direction are smaller than the largest examined initial gap sizes even for the highest examined level of ground motion.

5 CONCLUSIONS

Various configurations of a seat-type abutment-backfill model in the longitudinal and the transverse directions were studied, focusing on an existing overpass designed according to modern code provisions. From both the static and the dynamic (response history) analyses, it emerged that the performance of the bridge improved and that the response of its various components was different when the abutment-backfill system was taken into account, highlighting the importance of modelling this system. Specifically:

- ‘Hinging’ and shearing-off (‘fully sacrificial’) backwalls behave differently when the joint gap closes, hence their modelling should account for this. Abutment-backfill systems with shearing-off backwalls present higher initial stiffness and strength than the ones with ‘hinging’ backwalls; this occurs at the cost of early backwall damage, whereas they reach their strength peak at smaller displacements.
- A single nonlinear spring with a properly defined constitutive law based on passive pressures developing on the backfill is sufficient for modelling the shearing-off system. On the contrary, it is not appropriate for a ‘hinging’ backwall, where the nonlinear behaviour at its base differentiates the response of the entire abutment-backfill system. In this case the single-spring model must be based on the pushover curve derived from the analysis of the abutment-backfill component of the bridge, as described in this paper.
- Modelling the nonlinear behaviour of the backfill soil behind the stem wall of a seat-type abutment is not required, at least in the common case that the stem walls is much stiffer than the backwall, since that part of the soil barely deforms.
- The location of the springs that represent the backfill soil affects the calculated response of the abutment-backfill system, while their number also has some influence. For common backwalls of around 2 m height, use of three springs suffices.
- Modelling the gap element separately, which is necessary for response history analyses with the ‘detailed’ abutment-backfill model, is prone to cause numerical instabilities and/or long computation time. Use of constitutive law with an initial flat slope is clearly preferable, but is not available in all software packages.
- The bearings and the piers are generally relieved as the gap size is made smaller and hence the abutment-backfill system is activated; this occurs at the cost of increased response of the abutment-backfill system that may cause damage to the more critical component of this system.

REFERENCES

[1] Caltrans, “Seismic Design Criteria (version 2.0),” CA, USA, 2019.

[2] A. Shamsabadi, P. Khalili-Tehrani, J. P. Stewart, and E. Taciroglu, “Validated simulation models for lateral response of bridge abutments with typical backfills,” *Journal of Bridge Engineering*, **15**, no. 3, pp. 302–311, 2010.

[3] A. Aviram, K. R. Mackie, and C. Florida, “PACIFIC EARTHQUAKE ENGINEERING Guidelines for Nonlinear Analysis of Bridge Structures in California,” 2008.

[4] R. Omrani *et al.*, “Guidelines for Nonlinear Seismic Analysis of Ordinary Bridges: Version 2.0,” *Caltrans Final Report No. 15-65A0454*, no. December, p. 168, 2015.

[5] CEN (2005), “Eurocode 8: Design of Structures for Earthquake Resistance–Part 2: Bridges,” *European Committee for Standardization, Brussels*, 2005.

[6] CSI, “SAP2000 v.22: Integrated Software for Structural Analysis and Design.” CA, USA, 2020.

[7] T. Paulay and M. J. N. Priestley, *Seismic design of reinforced concrete and masonry buildings*. Wiley New York, 1992.

[8] D. Biskinis and M. N. Fardis, “Stiffness and cyclic deformation capacity of circular RC columns with or without lap-splices and FRP wrapping,” *Bulletin of Earthquake Engineering*, **11**, no. 5, pp. 1447–1466, 2013.

[9] V. K. Papanikolaou, “Analysis of arbitrary composite sections in biaxial bending and

axial load," *Computers & structures*, **98**, pp. 33–54, 2012.
[10] CEN (2004), "Eurocode 2: Design of concrete structures—Part 1-1: General rules and rules for buildings," *EN 1992-1-1*, 2004.
[11] R. Park and R. A. Sampson, "Ductility of reinforced concrete column sections in seismic design," in *Journal Proceedings*, 1972, **69**, no. 9, pp. 543–555.
[12] F. Naeim and J. M. Kelly, *Design of seismic isolated structures: from theory to practice*. John Wiley & Sons, 1999.
[13] G. Mylonakis, S. Nikolaou, and G. Gazetas, "Footings under seismic loading: Analysis and design issues with emphasis on bridge foundations," *Soil Dynamics and Earthquake Engineering*, **26**, no. 9, pp. 824–853, 2006.
[14] D. Biskinis, "Strength and deformation capacity of reinforced concrete members with or without strengthening," PhD Dissertation, University of Patras, 2007 (in Greek), 2007.
[15] P. Khalili-Tehrani, A. Shamsabadi, J. P. Stewart, and E. Taciroglu, "Backbone curves with physical parameters for passive lateral response of homogeneous abutment backfills," *Bulletin of Earthquake Engineering*, **14**, no. 11, pp. 3003–3023, 2016.
[16] A. Shamsabadi, K. M. Rollins, and M. Kapuskar, "Nonlinear soil–abutment–bridge structure interaction for seismic performance-based design," *Journal of geotechnical and geoenvironmental engineering*, **133**, no. 6, pp. 707–720, 2007.
[17] R. T. Cole and K. M. Rollins, "Passive earth pressure mobilization during cyclic loading," *Journal of Geotechnical and Geoenvironmental Engineering*, **132**, no. 9, pp. 1154–1164, 2006.
[18] I. M. Thomaidis, A. J. Kappos, and A. Camara, "Dynamics and seismic performance of rocking bridges accounting for the abutment-backfill contribution," *Earthquake Engineering & Structural Dynamics*, **49**, no. 12, pp. 1161–1179, Oct. 2020.
[19] Y. Xie, Y. Huo, and J. Zhang, "Development and validation of p-y modeling approach for seismic response predictions of highway bridges," *Earthquake Engineering & Structural Dynamics*, **46**, no. 4, pp. 585–604, 2017.
[20] CSI, "Analysis reference manual for SAP2000, ETABS, SAFE and CSIBridge," *Computers and Structures, Inc., Berkeley, CA, USA*, 2017.
[21] K. I. Gkatzogias and A. J. Kappos, "Direct estimation of seismic response in reduced-degree-of-freedom isolation and energy dissipation systems," *Earthquake Engineering and Structural Dynamics*, **48**, no. 10, pp. 1112–1133, 2019.
[22] G. Weatherill, H. Crowley, and L. Danciu, "Preliminary reference Euro-Mediterranean seismic hazard zonation," 2013.
[23] S.-H. Kim and M. Shinozuka, "Effects of Seismically Induced Pounding at Expansion Joints of Concrete Bridges," *Journal of Engineering Mechanics*, **129**, no. 11, pp. 1225–1234, 2003.